Proposal of Time Domain Channel Estimation Method for MIMO-OFDM Systems

Tanairat Mata[1(✉)], Pisit Boonsrimuang[2], Kazuo Mori[1], and Hideo Kobayashi[1]

[1] Graduate School of Engineering, Mie University, Tsu, 514-8507, Japan
tanairat@com.elec.mie-u.ac.jp,
{kmori,koba}@elec.mie-u.ac.jp
[2] Faculty of Engineering, King Mongkut's Institute of Technology Ladkrabang, Bangkok 10520, Thailand
kbpisit@kmitl.ac.th

Abstract. This paper proposes a time domain channel estimation (TD-CE) method for Multi Input Multi Output-Orthogonal Frequency Division Multiplexing (MIMO-OFDM) systems. The feature of proposed TD-CE method is to estimate channel frequency responses for all links between transmit and receive antennas in MIMO-OFDM systems by using one scattered pilot preamble symbol in the time domain. The proposed method can achieve higher channel estimation accuracy even when the number of transmission antennas is larger and the transmission signal is sampled by a non-Nyquist rate in which the number of IFFT points is different from the number of data subcarriers due to the insertion of null subcarriers (zero padding) at the both ends of data subcarriers. This paper shows various computer simulation results in the time-varying fading channels to demonstrate the effectiveness of the proposed channel estimation method as comparing with the conventional channel estimation methods.

Keywords: Time domain channel estimation (TD-CE) · MIMO · Channel impulse response · Channel frequency response · Non-Nyquist rate

1 Introduction

Orthogonal Frequency Division Multiplexing (OFDM) has been widely adopted in the current wireless communications systems as the standard transmission technique such as the Digital Audio and Video Broadcasting (DAB [1] and DVB [2]), Broadband Wireless Access (IEEE 802.16) [3] and Wireless Local Area Network (WLAN) [4] because of its efficient usage of frequency bandwidth and robustness to the multipath fading. Furthermore, the Multi Input Multi Output (MIMO) technique is employed with OFDM technique (MIMO-OFDM) [5] to achieve higher data transmission rate and higher signal quality in various wireless communication systems.

In MIMO-OFDM systems, the receiver needs to estimate the channel frequency responses (CFR) precisely for all links between transmit and receive antennas which are

P. Pillai et al. (Eds.): WiSATS 2015, LNICST 154, pp. 215–228, 2015.
DOI: 10.1007/978-3-319-25479-1_16

used in the demodulation of information data with the MIMO detection. From this fact, the channel estimation (CE) method which can achieve higher estimation accuracy is essential in MIMO-OFDM systems to achieve higher data transmission rate with keeping higher signal quality. Up to today, many CE methods have been proposed for MIMO-OFDM systems including the Discrete Fourier Transform interpolation-channel estimation (DFTI-CE) method [6] and the Maximum Likelihood-channel estimation (ML-CE) method [7]. The DFTI-CE method can achieve higher estimation accuracy only when the sampling rate of transmission signal is the Nyquist rate *i.e.* the number of IFFT points (N) is equal to the number of data subcarriers (M). However the estimation accuracy of DFTI-CE method would be degraded relatively in the practical MIMO-OFDM systems in which the sampling rate is taken by the non-Nyquist rate. In the practical OFDM system, the null subcarriers (zero padding) are usually inserted at the both ends of M data subcarriers in every transmission OFDM symbol to reject the aliasing occurring at the output of digital to analogue (D/A) converter. From this fact, the channel estimation accuracy of using this method would be degraded especially at around the both ends of data subcarriers which are the borders between the data and null subcarriers due to the mismatching of sampling rate between the transmission signal with N samples and received signal with M samples. This phenomenon is called the border effect [8]. To solve the above problem, the ML-CE method was proposed for the MIMO-OFDM systems which can achieve higher estimation accuracy than the conventional DFTI-CE method [7]. However its estimation accuracy at the both ends of data subcarriers would be degraded when increasing the number of transmit antennas.

To solve the above problems on the conventional CE methods, this paper proposes a novel channel estimation method which can achieve higher estimation accuracy even when the non-Nyquist rate and increasing the number of transmit antennas in the MIMO-OFDM systems. The salient feature of proposed TD-CE method is to employ the superimposed time domain received scattered pilot preamble (SPP) symbol sent from all the transmit antennas in which pilot subcarriers sent from each transmit antenna are assigned cyclically including the both ends of transmission frequency band for data subcarriers. In the proposed method, the channel frequency responses for all links between transmit and receive antennas are estimated over the frequency band corresponding from the first to the end pilot subcarriers of which frequency band is also used in the transmission of data information. This paper is organized as follows. Section 2 presents the conventional CE methods for MIMO-OFDM systems and their problems on the estimation accuracy at the non-Nyquist rate and when increasing the number of transmit antennas. Section 3 proposes the TD-CE method for MIMO-OFDM systems which can solve the problems on the conventional methods. Section 4 presents various computer simulation results to verify the effectiveness of proposed method and Sect. 5 draws some conclusions.

2 Conventional Channel Estimation Method

2.1 System Model for MIMO-OFDM Systems

For simplicity, we consider the MIMO-OFDM systems employing the Space Division Multiple Access (SDMA) technique with N_T transmit and N_R receive antennas

which enables the transmission of separate information data from each transmit antenna. Figure 1 shows a block diagram of MIMO-OFDM system with the SDMA. At the transmitter, the information data encoded by FEC is modulated and separated by M subcarriers into each transmit antenna. The zero padding are added at the both ends of M data subcarriers then converted into the time domain signal by N points IFFT at each transmit antenna. The time domain signal b_k^i at the k-th time sample ($0 \le k \le N\text{-}1$) transmitted from the T_i transmit antenna ($1 \le i \le N_T$) is sent to the receive antenna R_j ($1 \le j \le N_R$) after adding the guard interval (GI) to avoid the inter symbol interference (ISI). At the receiver, the data information transmitted from N_T transmit antennas are demodulated by using the MIMO detection with the estimated channel frequency response matrix consisting of all links between transmit and receive antennas.

In the MIMO-OFDM systems, ($N_T \times N_R$) channels between transmit and receive antennas are required to estimate by using one common SPP symbol. Figure 2 shows an example of pilot subcarriers assignment in the SPP symbol sent from the i-th transmit antenna. In the Fig. 2, N is the number of IFFT points, M is the number of data subcarriers, (N-M) represents the total number of null subcarriers (zero padding) and the half of the null subcarriers (N-M)/2 are inserted at both ends of M data subcarrier. Each transmit antenna can use P ($=M/K_f$) pilot subcarriers within M subcarrier which are inserted cyclically with an interval of K_f subcarrier. J represents the first data subcarrier number ($J=(N\text{-}M)/2$) within N subcarriers including the zero padding. The pilot subcarriers for the i-th transmit antenna are assigned from $J+(i\text{-}1)$ to $J+(i\text{-}1)+sK_f$ ($0 \le s \le P\text{-}1$) with the interval of K_f subcarriers. Here it should be noted that the pilot subcarriers sent from each transmit antenna are assigned cyclically so as to avoid a collision among the pilot subcarriers sent from all transmit antennas. The time domain SPP symbol b_k^i transmitted from the i-th transmit antenna is given by,

$$b_k^i = \frac{1}{N} \cdot \sum_{s=0}^{P-1} B_s^i \cdot e^{j\frac{2\pi k}{N}(J+(i-1)+sK_f)}, \quad (0 \le k \le N-1) \tag{1}$$

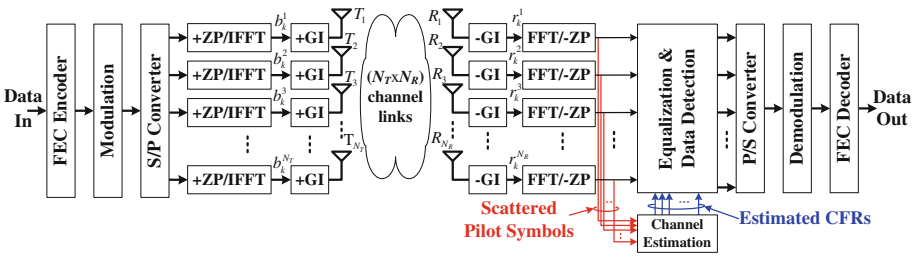

Fig. 1. Overview of MIMO-OFDM system.

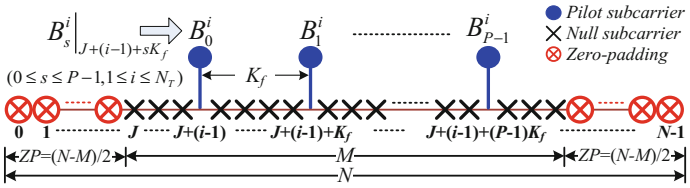

Fig. 2. Assignment of pilot subcarriers in SPP symbol.

Where B_s^i is the s-th pilot data for the i-th transmit antenna of which subcarrier number is $J+(i\text{-}1)+sK_f$ within N subcarriers. The channel impulse response (CIR) of multipath fading between the i-th transmit and the j-th receive antennas can be expressed by,

$$h_k^{i,j} = \sum_{q(i,j)=0}^{N_P-1} \rho_{q(i,j)}^{i,j} \cdot \delta\left(k - q(i,j)\right) \tag{2}$$

where N_P is the number of delay paths and $\rho_{q(i,j)}^{i,j}$ represents the complex amplitude of CIR for the $q(i,j)$-th delay path occurred in the channel between the i-th transmit and j-th receive antennas. At the j-th receive antenna, the superimposed received SPP signal r_k^j sent from all transmit antennas after removing the GI can be given by,

$$r_k^j = \sum_{i=1}^{N_T} \left\{ b_k^i \otimes h_k^{i,j} \right\} + z_k^j = \sum_{i=1}^{N_T} \sum_{q(i,j)=0}^{N_P-1} \left\{ \rho_{q(i,j)}^{i,j} \cdot b_{k-q(i,j)}^i \right\} + z_k^j, \quad \left(1 \le j \le N_R\right) \tag{3}$$

where z_k^j is the additive white Gaussian noise (AWGN) at the k-th time sample of j-th receive antenna and $\otimes$ represents the convolution. The CFR at the pilot subcarriers between the i-th transmit and j-th receive antennas can be estimated independently by using the superimposed frequency domain received SPP symbol which is converted from the time domain signal in (3), because the pilot subcarriers sent from all transmit antennas are assigned without a collision as described above. By performing FFT to (3), the received frequency domain SPP symbol at the $J+(i\text{-}1)+sK_f$-th pilot subcarrier is given by,

$$R_{J+(i-1)+sK_f}^j = B_s^i \sum_{q(i,j)=0}^{N_P-1} \rho_{q(i,j)}^{i,j} e^{-j\frac{2\pi q(i,j)}{N}(J+(i-1)+sK_f)} + Z_{J+(i-1)+sK_f}^j = B_s^i H_{J+(i-1)+sK_f}^{i,j} + Z_{J+(i-1)+sK_f}^j \tag{4}$$

where $H_{J+(i-1)+sK_f}^{i,j}$ and $Z_{J+(i-1)+sK_f}^j$ are the CFR at the $J+(i\text{-}1)+sK_f$-th pilot subcarrier between the i-th transmit and j-th receive antennas and AWGN at the j-th receive antenna both in the frequency domain. From (4), the CFR $H_{J+(i-1)+sK_f}^{i,j}$ can be estimated by using the pilot data B_s^i known at the receiver which is given by,

$$\hat{H}^{i,j}_{J+(i-1)+sK_f} = \frac{R^j_{J+(i-1)+sK_f}}{B^i_s} = H^{i,j}_{J+(i-1)+sK_f} + \frac{Z^j_{J+(i-1)+sK_f}}{B^i_s} \tag{5}$$

The next section presents the conventional DFTI-CE and ML-CE methods by using the estimated CFR at the pilot subcarriers given in (5).

2.2 Conventional DFTI-CE Method

The DFT-CE method has been proposed for MIMO-OFDM systems [6] which can achieve higher channel estimation accuracy by reducing the noise component in the time domain CIR. By performing P points IDFT to (5), the CIR $\hat{g}^{i,j}_u$ is given by,

$$\hat{g}^{i,j}_u = \frac{1}{P} \cdot \sum_{s=0}^{P-1} \hat{H}^{i,j}_{J+(i-1)+sK_f} \cdot e^{j\frac{2\pi su}{P}} = g^{i,j}_u + w^{i,j}_u, \quad (0 \le u \le P-1) \tag{6}$$

where $g^{i,j}_u$ in (6) is the ideal CIR for $H^{i,j}_{J+(i-1)+sK_f}$ in (5) and $w^{i,j}_u$ is the noise component both at the u-th time sampling. By using (4), the ideal CIR $g^{i,j}_u$ is given by,

$$g^{i,j}_u = \frac{1}{P} \cdot \sum_{q(i,j)=0}^{N_P-1} \rho^{i,j}_{q(i,j)} \cdot e^{-j\frac{2\pi q(i,j)}{N}(J+i-1)} \cdot \sum_{s=0}^{P-1} e^{-j\frac{2\pi s}{P}(\frac{PK_f}{N}q(i,j)-u)} \tag{7}$$

When N is equal to M ($=PK_f$) at the Nyquist rate, the last term in (7) is given by [9],

$$\sum_{s=0}^{P-1} e^{-j\frac{2\pi s}{P}(\frac{PK_f}{N}q(i,j)-u)} = \sum_{s=0}^{P-1} e^{-j\frac{2\pi s}{P}(q(i,j)-u)} = \begin{cases} P, & q(i,j) = u \\ 0, & q(i,j) \ne u \end{cases} \tag{8}$$

By inserting (8) into (7), the CIR $g^{i,j}_u$ exists only from u=0 to N_P-1 which is the same as (2). From this fact, the noise components from u=N_P to P-1 can be removed by adding zeros and then the CFR over M data subcarriers can be estimated precisely by performing M points DFT to (6). However when N is larger than M (N>M) due to the insertion of zero padding at the both ends of M data subcarriers which corresponds to the non-Nyquist rate, the last term of (7) can be given by,

$$\sum_{s=0}^{P-1} e^{-j\frac{2\pi s}{P}(\frac{PK_f}{N}q(i,j)-u)} = \frac{1 - e^{-j2\pi(\frac{PK_f}{N}q(i,j)-u)}}{1 - e^{-j\frac{2\pi}{P}(\frac{PK_f}{N}q(i,j)-u)}} \tag{9}$$

By inserting (9) into (7), the CIR $g^{i,j}_u$ exists over P time sampling points from u=0 to P-1 which is completely different from the ideal CIR given in (2). From this fact, the channel estimation accuracy of using the DFTI-CE method at the non-Nyquist rate would be degraded relatively especially at the borders between the zero padding and data subcarriers.

2.3 Conventional ML-CE Method

To improve the border effect in the DFTI-CE method at the non-Nyquist rate, the ML-CE method was proposed [7]. In the ML-CE method, the CIR $\hat{\rho}^{i,j}_{q(i,j)}$ can be estimated by the following Maximum Likelihood (ML) equation [10].

$$L_{ML}\left\langle \hat{\rho}^{i,j}_{q(i,j)} \right\rangle = \arg\min_{\hat{\rho}^{i,j}_{q(i,j)}} \left[\sum_{s=0}^{P-1} \left| \sum_{q(i,j)=0}^{Ng-1} \rho^{i,j}_{q(i,j)} \cdot e^{-j\frac{2\pi q(i,j)}{N}(J+(i-1)+sK_f)} - \hat{H}^{i,j}_{J+(i-1)+sK_f} \right|^2 \right] \tag{10}$$

The ML equation given in (10) can be expressed by the following simultaneous equations.

$$\left\| \hat{\rho}^{i,j}_{q(i,j)} \right\|_{Ng\times 1} = \dagger \left\| D^{i,j}_{q(i,j),J+(i-1)+sK_f} \right\|_{p\times Ng} \cdot \left\| \hat{H}^{i,j}_{J+(i-1)+sK_f} \right\|_{p\times 1} \tag{11}$$

where † denotes the Moore-Penrose pseudo inverse matrix, $\left\| \hat{\rho}^{i,j}_{q(i,j)} \right\|$ is the matrix of the complex amplitude of CIR with the matrix size [$Ng\times1$], and $\left\| D^{i,j}_{q(i,j),J+(i-1)+sK_f} \right\|$ with the matrix size [$P\times Ng$] can be given by,

$$D^{i,j}_{q(i,j),J+(i-1)+sK_f} = e^{-j\frac{2\pi q(i,j)}{N}(J+(i-1)+sK_f)}, \quad (0 \le q(i,j) \le Ng-1) \tag{12}$$

Since the number of actual delay paths N_P is unknown at the receiver, the length of GI (Ng) is used in the estimation of CIR in (10). After performing DFT to (11), the CFR can be estimated over M data subcarriers. Although the ML-CE method can improve the border effect and achieve higher channel estimation accuracy, its estimation accuracy at the both ends of data subcarriers would be degraded when increasing the number of transmit antennas [7]. When increasing the number of transmit antennas, the interval of pilot subcarriers K_f becomes larger and the number of subcarriers which are not covered by pilot subcarriers at the both ends of M data subcarriers are increased as shown in Fig. 2. This is the reason that the estimation accuracy of ML-CE method obtained by (10) would be degraded when increasing the number of antennas.

3 Proposal of Time Domain Channel Estimation Method

To solve the above problems having the conventional DFTI-CE and ML-CE methods, this section proposes a time domain-channel estimation (TD-CE) method by using one SPP symbol which can improve the border effect even when the non-Nyquist rate and increasing the number of transmit antennas.

3.1 Proposed Pilot and Data Subcarriers Assignment Method

Figure 3(a) shows the proposed pilot subcarriers assignment for the SSP symbol sent from the i-th transmit antenna. In the Fig. 3, the pilot subcarriers are inserted with the interval of K_f subcarriers starting from the $J+(i\text{-}1)$-th to the $J+(i\text{-}1)+(P\text{-}1)K_f$-th subcarriers which covers the bandwidth of $M_p=M\text{-}N_T+1$. Here it should be noted that the frequency band covered by both ends of pilot subcarriers for the i-th transmit antenna is different from other transmit antennas and the data subcarriers are assigned within the same bandwidth of M_p subcarriers between the first to the end pilot subcarriers as shown in Fig. 3(b). In the proposed pilot assignment method, the active number of data subcarriers becomes $M_p=M\text{-}N_T+1$ which is smaller number than M for the conventional method as shown in Fig. 2. However, it can be expected that channel estimation accuracy at around the borders between the null subcarriers and data subcarriers could be better than the conventional method because the pilot subcarriers are inserted at the both ends of data subcarriers.

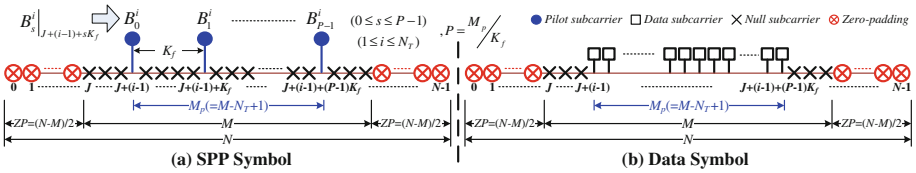

Fig. 3. Proposed pilot and data subcarriers assignment for i-th transmit antenna.

3.2 Proposed Time Domain Channel Estimation (TD-CE) Method

This section proposes the TD-CE method by using the proposed pilot and data assignment method as shown in Fig. 3 which can achieve higher estimation accuracy at around the borders between the data and zero padding subcarriers even when the Non-Nyquist rate and when increasing the number of transmit antennas. Accordingly, it can be expected that the proposed TD-CE method can achieve better BER performance than those for the conventional DFTI-CE and ML-CE methods.

The superimposed received SPP symbol r_k^j at the j-th receive antenna can be given by the following equation in which the received SPP symbol sent from each transmit antenna to the j-th receive antenna is expressed separately.

$$r_k^j = \underbrace{\sum_{q(1,j)=0}^{Ng-1} \rho_{q(1,j)}^{1,j} \cdot b_{k-q(1,j)}^{i}}_{from\ T_1\ to\ R_j} + \cdots + \underbrace{\sum_{q(N_T,j)=0}^{Ng-1} \rho_{q(N_T,j)}^{N_T,j} \cdot b_{k-q(N_T,j)}^{N_T}}_{from\ T_{N_T}\ to\ R_j} + z_k^j \tag{13}$$

The length of GI Ng in (13) is usually taken by longer than the N_P so as to avoid the Inter-symbol interference (ISI). By using the matrix multiplication, (13) can be rewritten by,

$$\mathrm{r} = \underbrace{\begin{bmatrix} \ddot{\mathrm{r}}_0^1 & \ddot{\mathrm{r}}_{-1}^1 & \cdots & \ddot{\mathrm{r}}_{1-N\geq}^1 \\ \ddot{\mathrm{r}}_1^1 & \ddot{\mathrm{r}}_0^1 & \cdots & \ddot{\mathrm{r}}_{2-N\geq}^1 \\ \vdots & \vdots & \ddots & \vdots \\ \ddot{\mathrm{r}}_N^1 & \ddot{\mathrm{r}}_{N-\natural}^1 & \cdots & \ddot{\mathrm{r}}_{N-N\geq}^1 \end{bmatrix}}_{\mathrm{b}_1} \cdot \underbrace{\begin{bmatrix} \ddot{\mathrm{r}}_0^{\natural,} \\ \ddot{\mathrm{r}}_1^{\natural,} \\ \vdots \\ \ddot{\mathrm{r}}_{N\geq-1}^{\natural,} \end{bmatrix}}_{\mathrm{c}_{1,\mathrm{j}}} + \ldots + \underbrace{\begin{bmatrix} \ddot{\mathrm{r}}_0^{N_T} & \ddot{\mathrm{r}}_{-1}^{N_T} & \cdots & \ddot{\mathrm{r}}_{1-Ng}^{N_T} \\ \ddot{\mathrm{r}}_1^{N_T} & \ddot{\mathrm{r}}_0^{N_T} & \cdots & \ddot{\mathrm{r}}_{2-Ng}^{N_T} \\ \vdots & \vdots & \ddots & \vdots \\ \ddot{\mathrm{r}}_N^{N_T} & \ddot{\mathrm{r}}_{N-1}^{N_T} & \cdots & \ddot{\mathrm{r}}_{N-Ng}^{N_T} \end{bmatrix}}_{\mathrm{b}_{\mathcal{N}}} \cdot \underbrace{\begin{bmatrix} \rho_0^{N_T,} \\ \rho_1^{N_T,} \\ \vdots \\ \rho_{N\geq-1}^{N_T,} \end{bmatrix}}_{\mathrm{c}_{\mathcal{N},}} + \mathrm{z} \tag{14}$$

where $\mathbf{r}_j$ is the matrix of received signal r_k^j with the matrix size [N×1], $\mathbf{b}_i$ and $\mathbf{c}_{i,j}$ are the matrix of time domain SPP symbol b_k^i with the matrix size [N×Ng] and the matrix of complex amplitude of CIR $h_k^{i,j}$ with the matrix size [Ng×1] and $\mathbf{z}_j$ is the matrix of AWGN z_k^j with the matrix size [N×1]. The matrix operation of (14) at the j-th receive antenna is rewritten by,

$$\mathbf{r}_j = \underbrace{\mathbf{b}_1 \cdot \mathbf{c}_{1,j}}_{from\ T_1\ to\ R_j} + \cdots \underbrace{\mathbf{b}_{N_T} \cdot \mathbf{c}_{N_T,j}}_{from\ T_{N_T}\ to\ R_j} + \mathbf{z}_j = \underbrace{[\mathbf{b}_1 \cdots \mathbf{b}_{N_T}]}_{\mathbf{B}} \cdot \underbrace{[\mathbf{c}_{1,j} \cdots \mathbf{c}_{N_T,j}]^T}_{\mathbf{G}_j} + \mathbf{z}_j = \mathbf{B} \cdot \mathbf{G}_j + \mathbf{z}_j \tag{15}$$

where $[\ ]^{\mathrm{T}}$ is the transpose matrix operation. $\mathbf{B}$ is the matrix of time domain SPP symbol $\mathbf{b}_i$ sent from all transmit antennas with the matrix size [N_R×$N_T Ng$] and $\mathbf{G}_j$ is the matrix of CIR $\mathbf{c}_{i,j}$ for all links from all transmit antennas to the j-th receive antenna with the matrix size [$N_T Ng$×1]. From (15), the CIRs in matrix $\mathbf{G}_j$ can be estimated by using the Moore-Penrose pseudo inverse $\mathbf{B}^{\dagger}$ which can be given by,

$$\hat{\mathbf{G}}_j = \mathbf{B}^{\dagger} \cdot \mathbf{r}_j = \mathbf{G}_j + \mathbf{B}^{\dagger} \cdot \mathbf{z}_j \tag{16}$$

All CIRs can be estimated together by using (16) in the time domain at the j-th receive antenna. Since all the time domain SPP symbols sent from all transmit antennas are known at the receiver, $\mathbf{B}^{\dagger}$ can be calculated in advance at the receiver. From this fact, the estimation of CIRs for all links can be estimated by simple matrix multiplication as given in (16) which leads the considerable reduction of computational complexity in the proposed TD-CE method. In the time varying fading channels, the SPP symbols are inserted with the interval of K_t symbols in one frame and the CIRs over one frame can be estimated by applying the cubic interpolation method to the CIRs estimated at the SPP symbols with the interval of K_t symbols by (16). The CFRs for all links over one frame can be obtained by performing DFT to the estimated CIRs. Finally, the information data in one OFDM frame can be demodulated precisely by the MIMO detection of using the estimated CFR matrix even in higher time-varying fading channel.

4 Performance Evaluations

This section presents various computer simulation results to verify the effectiveness of proposed TD-CE method in the time-varying fading channel. Table 1 shows the simulation parameters used in the following evaluations.

Table 1. Simulation parameters.

Parameters	Values
Modulation method for data subcarriers	16QAM
Modulation method for pilot subcarriers	QPSK
No. of FFT points (N)	128
No. of data subcarriers in conv. methods (M)	96
No. of data subcarriers in proposed methods (M_p)	M-N_T+1
Length of GI (Ng)	11
OFDM frame length (L-Symbols)	17
Interval of pilot in freq. (K_f) and in time (K_t) axes	$K_f = N_T$ and K_t=4
No. of transmit and receive antennas ($N_T \times N_R$)	4×4 and 8×8
OFDM occupied bandwidth (BW)	5 MHz
Radio frequency (f_c)	2 GHz
Forward Error Correction (FEC) Code	
-Encoding	Convolution (R=1/2, K=7)
-Decoding	Hard-decision withViterbi
-Interleaver	Matrix with one frame (L)
-Packet length (information bits/packet)	512 bits
Multipath Rayleigh fading channel model	
-Delay profile	Exponential
-Decay constant	-1 dB
-No. of delay paths (N_P) in all links	10
-No. of scattered rays	20

Figure 4 shows the normalized mean square error (NMSE) performances of estimated CFR evaluated at each subcarrier for the proposed TD-CE, Conv.DFTI-CE and Conv.ML-CE methods when the sampling rate are taken by the Nyquist rate (N=M) and non-Nyquist (N≠M) rate. The number of transmit (N_T) and receive (N_R) antennas are 8×8. From the figure, it can be seen that there is no border effect in the NMSE performances for all CE methods when the sampling rate is the Nyquist rate. When the sampling rate is the non-Nyquist rate, the proposed TD-CE methods has no border effects while the Conv.DFTI-CE and Conv. ML-CE methods have the border effects at around the

both ends of data subcarriers. From these results, it can be concluded that the proposed TD-CE method can achieve higher estimation accuracy even when the non-Nyquist rate and the larger number of transmit antennas.

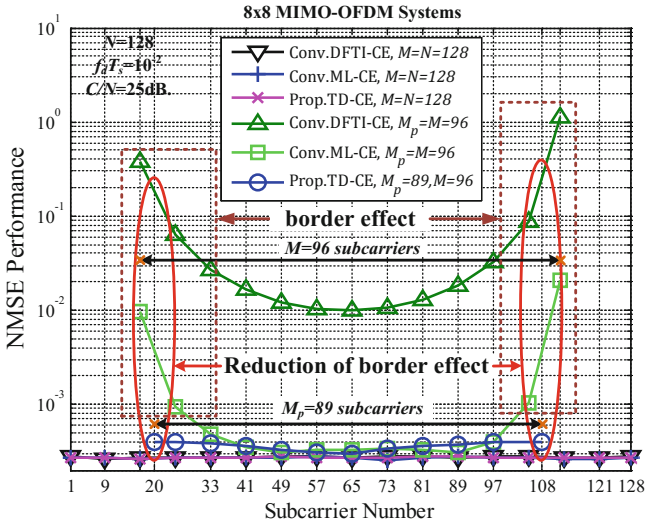

Fig. 4. CFR estimation accuracy for proposed method at each subcarrier.

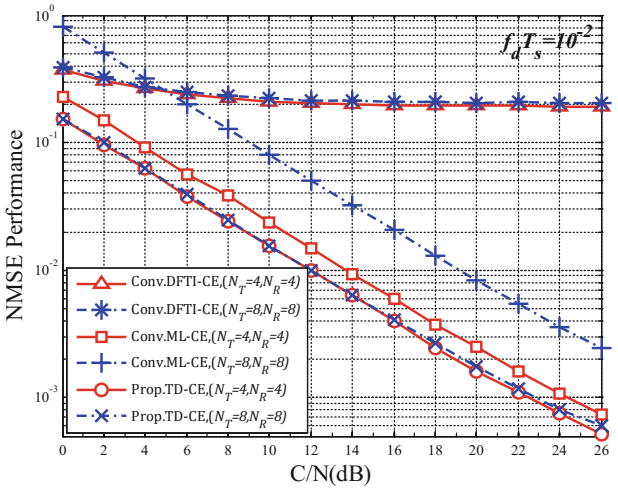

Fig. 5. CFR estimation accuracy for proposed method versus C/N(dB) at non-Nyquist rate.

Figure 5 shows the NMSE performance of estimated CFR when changing the carrier to noise power ratio (C/N) for the proposed TD-CE, Conv.DFTI-CE and Conv.ML-CE methods at the non-Nyquist rate. In the evaluation, the number of transmit and receive

antennas ($N_T \times N_R$)=4×4 and 8×8, and the normalized Doppler frequency ($f_d T_s$) is 10^{-2} where f_d is the maximum Doppler frequency and T_s is the OFDM symbol duration including the guard interval (GI). From the figure, it can be seen that the NMSE performance for the Conv.DFTI-CE method is degraded relatively due to the border effect at the non-Nyquist rate. The performance for the Conv.ML-CE method is degraded when increasing the number of transmit antennas. The proposed TD-CE method shows higher estimation accuracy regardless of the number of transmit antennas than that for the Conv.ML-CE method.

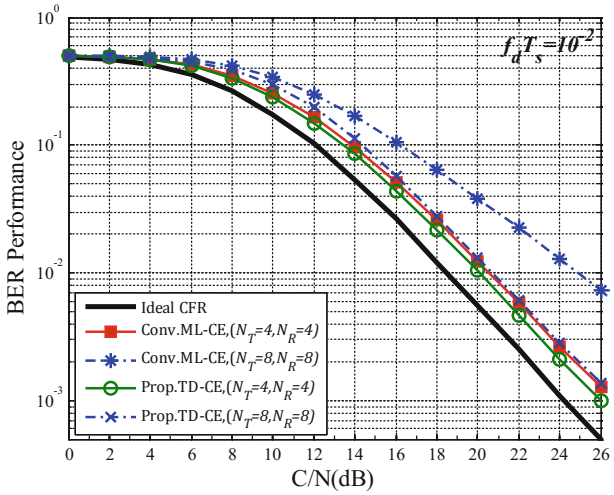

Fig. 6. BER performance for proposed method versus C/N(dB) at $f_d T_s = 10^{-2}$.

Figure 6 shows the BER performances when changing C/N at $f_d T_s = 10^{-2}$ for the Conv.ML-CE and proposed TD-CE methods at the non-Nyquist rate. From the figure, it can be seen that both 4×4 and 8×8 MIMO-OFDM systems with the proposed TD-CE method shows better BER performance than those for the Conv.ML-CE method especially when the number of transmit antennas is 8. The degradation of BER performance for the Conv.ML-CE method as compared with the proposed TD-CE method is come from the degradation of channel estimation accuracy as shown in Fig. 5.

Table 2 shows the comparison of computation complexity required in one CFR estimation for the proposed and conventional methods when ($N_T \times N_R$) = 8×8. From Table 2, it can be observed that the computation complexity for the proposed TD-CE method is slightly larger than the Conv.DFTI-CE and Conv.ML-CE methods. From Table 2 and Figs. 5 and 6, it can be concluded that the proposed TD-CE method can achieve higher estimation accuracy and accordingly better BER performance than the conventional DFTI-CE and ML-CE methods with keeping almost the same computational complexity.

Table 2. Comparison of computational complexity for channel estimation methods.

Channel Estimation Methods	Computational complexity required in one channel estimation (N_T=8)	
Conv.DFTI-CE	$N \bullet log_2 N + P + P^2 + M \bullet P$	2,204
Conv.ML-CE	$N \bullet log_2 N + P + P^2 + M \bullet Ng$	2,108
Prop.TD-CE (M_p=M-N_T+1)	$N \bullet Ng + M_p \bullet Ng$	2,387

The throughput (*Thp*) performances defined by bps/Hz for the proposed and conventional methods are evaluated by using the following equation.

$$Thp = n_{bit} \cdot R \cdot N_T \cdot \frac{N}{N+Ng} \cdot \frac{M_p}{M} \cdot \frac{(L-1)(K_t-1)}{L \cdot K_t} \cdot (1 - PER), \quad (bps/Hz) \tag{17}$$

where n_{bit} is the modulation level (n_{bit}=4 for 16QAM), M_p (=M-N_T+1) is the number of active data subcarrier for the proposed method (M_p=M for conventional methods), R is the FEC rate, K_t is the interval of SPP symbol in the time axis, L is the frame length and *PER* is the packet error rate when the packet length (information bits/packet) is 512 bits. From (17) it can be seen that the throughput performance for the proposed method would be decreased by (M_p/M) due to the smaller number of active data subcarriers M_p (=M-N_T+1) which depends on the number of transmit antennas (N_T). However the NMSE estimation accuracy of proposed method is higher than the conventional ML-CE method as shown in Fig. 5 and accordingly the proposed method can achieve better BER performances as shown in Fig. 6. Consequently, the PER performance in (17) for the proposed TD-CE method becomes better than the conventional ML-CE method. From these reasons, it can be expected that the proposed TD-CE method can achieve higher throughput efficiency even when the number of active data subcarriers M_p for the proposed method is smaller than M that for the conventional ML-CE method.

Figure 7 shows the throughput performances for the Conventional ML-CE and proposed TD-CE methods evaluated by using (17). In the figure, the Ideal throughput performance which is given by assuming the ideal CFR for the Conv.ML-CE method is also shown as for the purpose of comparison with other methods. From the figure, it can be seen that the throughput performance for the proposed TD-CE method is almost the same as the Conv.ML-CE method when (N_T×N_R) = 4×4. This is the reason that the improvement of PER performance by using the proposed TD-CE method is not enough to compensate the reduction of ratio (M_p/M =93/96) for active data subcarriers in (17). However the throughput performance for the proposed method is much higher than the Conv.ML-CE method when (N_T×N_R) = 8×8. The throughput performances for the Conv.ML-CE and proposed TD-CE methods at C/N=30 dB are 2.6bps/Hz and 7.6bps/Hz, respectively which corresponds to the improvement of 5bps/Hz by the proposed TD-CE method.

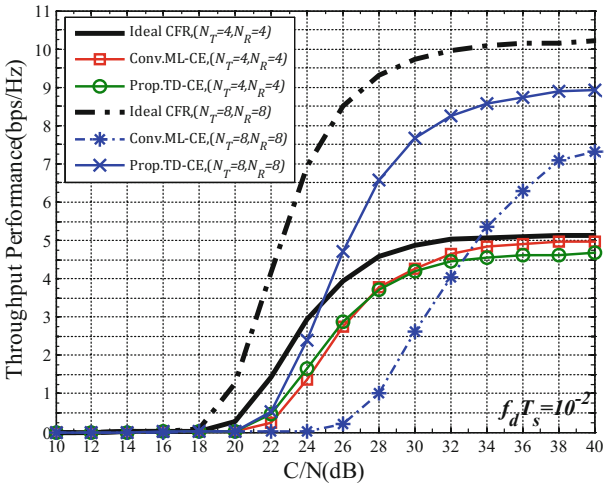

Fig. 7. Throughput performance for proposed method versus *C/N*(dB) at f_dT_s=10^{-2}.

This means that the proposed TD-CE method can achieve the transmission data rate of 38Mbps which is higher transmission data rate by 25Mbps than the Conv.ML-CE method of 13Mbps when the allocated frequency bandwidth is 5 MHz.

5 Conclusions

This paper proposed the time domain channel estimation (TD-CE) method for the MIMO-OFDM systems. The salient feature of proposed TD-CE method is to employ the scattered pilot preamble symbol in which pilot subcarriers sent from each transmit antenna are assigned cyclically including the both ends of transmission frequency band for data subcarriers. In the proposed method, the channel frequency responses for all links between transmit and receive antennas are estimated over the frequency band between the first to the end pilot subcarriers assigned for each transmit antenna. The same frequency band assigned for pilot subcarriers in each transmit antenna is also used in the transmission of data information. From the computer simulation results, it was confirmed that the MIMO-OFDM systems with the proposed TD-CE method can achieve higher throughput performance in higher time-varying fading channel with keeping almost the same computational complexity as comparing with the conventional methods even when the non-Nyquist rate and the larger number of transmit antennas.

Acknowledgments. The authors would like to thank to the Japanese Government (Monbukagakusho:MEXT) Scholarships who supported this research.

References

1. Radio Broadcasting Systems; Digital Audio Broadcasting (DAB) to mobile, portable and fixed receivers, ETS 300 401, v1.4.1 (2006)
2. Digital Video Broadcasting (DVB); Implementation guidelines for the second generation digital terrestrial television broadcasting system (DVB-T2), ETSI TS 102 831, v1.2.1 (2012)
3. IEEE Standard for Local and Metropolitan Area Networks Part 16: Air Interface for Fixed Broadband Wireless Access Systems. IEEE Std. 802.16 (2004)
4. Kim, J., Lee, I.: 802.11 WLAN history and new enabling MIMO techniques for next generation standards. IEEE Commun. Mag. **53**(3), 134–140 (2015)
5. Jiang, M., Hanzo, L.: Multi-user MIMO-OFDM for next generation wireless systems. Proc. IEEE **95**(7), 1430–1469 (2007)
6. Sure, P., Bhuma, C.M.: A pilot aided channel estimator using DFT based time interpolation for massive MIMO-OFDM systems. Int. J. Electron. Commun. AEU **69**(1), 321–327 (2015)
7. Mata, T., Boonsrimuang, P., Mori, K., Kobayashi, H.: Time-Domain channel estimation method for MIMO-OFDM systems. In: IEICE General Conference 2015, B-1-155 (2015)
8. Diallo, D., Helard, M., Cariou, L., Rabineau, R.: DFT based channel estimation methods for MIMO-OFDM systems. In: Vehicular Technologies: Increasing Connectivity, pp. 97–114 (2011)
9. Mata, T., Hourai, M., Boonsrimuang, P., Mori, K., Kobayashi, H.: Time domain channel estimation method for uplink OFDMA system. In: the 22nd International Conference on Telecommunications, ICT2015 (2015)
10. Kobayashi, H., Mori, K.: Proposal of channel estimation method for OFDM systems under time-varying fading environments. IEICE Trans. Comm. (Japanese edition) **J90-B**(12), 1249–1262 (2007)